Monatshefte für Chemie 137, 1225–1240 (2006)
DOI 10.1007/s00706-006-0515-z

Monatshefte für Chemie
Chemical Monthly
Printed in Austria

Pentamidine Analogs: Syntheses, Structures in Solid State by ^{13}C CP/MAS NMR Spectroscopy, and X-Ray Crystallography and their Preliminary Biological Screening Against Human Cancer

Dorota Maciejewska[1,*], **Paweł Kaźmierczak**[1], **Jerzy Żabiński**[1], **Irena Wolska**[2], and **Sylwia Popis**[1]

[1] Department of Organic Chemistry, Faculty of Pharmacy, Medical University of Warsaw, Warsaw, Poland
[2] Department of Crystallography, Faculty of Chemistry, Adam Mickiewicz University, Poznań, Poland

Received February 2, 2006; accepted March 7, 2006
Published online August 24, 2006

Summary. The synthesis of four new 1,5-bis(4-amidinophenoxy)-3-oxapentane analogs is described. The structures of the obtained bis-amidines and bis-nitriles in the solid state are evaluated on the basis of ^{13}C CP/MAS NMR spectra and theoretical calculations at DFT level. A single crystal X-ray diffraction structure is presented for 1,5-bis(4-amidinophenoxy)-3-oxapentane. A preliminary anti-cancer assay against three cell lines is also given.

Keywords. Amidines; NMR spectroscopy; X-Ray diffraction; Theoretical calculations.

Introduction

Aromatic bis-amidine compounds exhibit a wide range of activities against a number of pathogens [1], but only 1,5-bis(4-amidinophenoxy)pentane (pentamidine) is in widespread clinical use against *Pneumocystis carinii* pneumonia (*PC*P) [2, 3]. Because of an increasing number of immunosuppressed patients that could be infected by *Pneumocystis carinii* the current therapies against *PC*P need to be improved. In a large number of patients undergoing treatment with pentamidine there have commonly been drug-related toxicities demanding further search for new pentamidine analogs that have the desired potency and suitable bioavailability, but lost

* Corresponding author. E-mail: domac@farm.amwaw.edu.pl

their toxicity. Moreover, pentamidine and its analogs together with a number of other diamidines were evaluated for their anticancer, antiviral, and anticoagulant activity [4–8]. The importance of these compounds not only as the anti-*PC*P chemotherapeutics but also in these other venues indicates an underdeveloped potentially important class of compounds.

The biological activity of pentamidine and its analogs is closely related to their interaction with *DNA* at the adenine-thymine rich region in the minor-groove. Crystallographic studies of *DNA*-pentamidine complexes are useful tools for designing analogs [9–11].

This paper reports the syntheses, structural data, and a preliminary anticancer assay of the pentamidine analogs **1**–**4** (Fig. 1). Up to now, no systematic studies of pentamidine analogs in the solid state have been performed. Thus, we used the ^{13}C CP/MAS NMR technique and theoretical calculations of relevant shielding constants at DFT level of theory to obtain information about the structure and dynamic events in the solid state of the title compounds. The X-ray structure of 1,5-bis(4-amidinophenoxy)-3-oxapentane (**1**) is also presented and compared with its *DNA* complex [10].

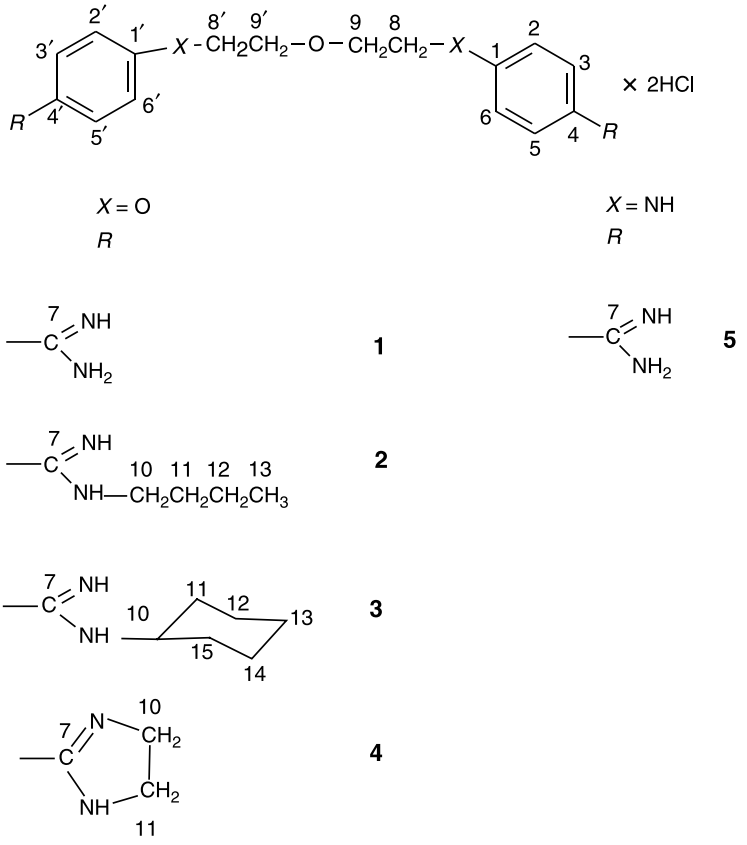

Fig. 1. Chemical formulae and atom numbering

Results and Discussion

Syntheses

The method of preparation of the diamidines generally followed the established route [12–14], which involves the preparation of the dinitriles and their subsequent conversion into diamidines. 1,5-Bis(4-amidinophenoxy)-3-oxapentane (**1**) was synthesized according to previous reports [15]. The previously unknown *N*-alkyl derivatives of 1,5-bis(4-amidinophenoxy)-3-oxapentane **2**–**4** were obtained in the course of a three-step synthesis (Scheme 1). It involves O-alkylation of 4-hydroxybenzonitrile with bis(2-chloroethyl)ether, then conversion of the formed 1,5-bis(4-cyanophenoxy)-3-oxapentane (**1b**) [15] to 1,5-bis[4-(ethoxyiminoyl)phenoxy]-3-oxapentane (**1c**). The latter was treated with appropriate amines (butylamine, cyclohexylamine, ethane-1,2-diamine) to yield the *N*-alkyl derivatives **2**–**4**. The new compounds **5b** and **5** were prepared by modification of this procedure (Scheme 2). 4-Fluorobenzonitrile was obtained from commercially available 4-fluorobenzaldehyde by refluxing its formic acid solution with hydroxylamine hydrochloride [16]. 1,5-Diamino-3-oxapentane was prepared from bis(2-chloroethyl) ether by *Gabriel* synthesis [17]. The N,N-dialkylation of 1,5-diamino-3-oxapentane with 4-fluorobenzonitrile resulted in the dinitrile **5b**. It was converted to the diamidine **5** as described for **1**.

X-Ray Structure of 1,5-Bis[4-amidinophenoxy]-3-oxapentane (**1**)

The crystal and molecular structures of **1** were determined by single crystal X-ray diffraction. The crystallographic data, together with data collection and structure

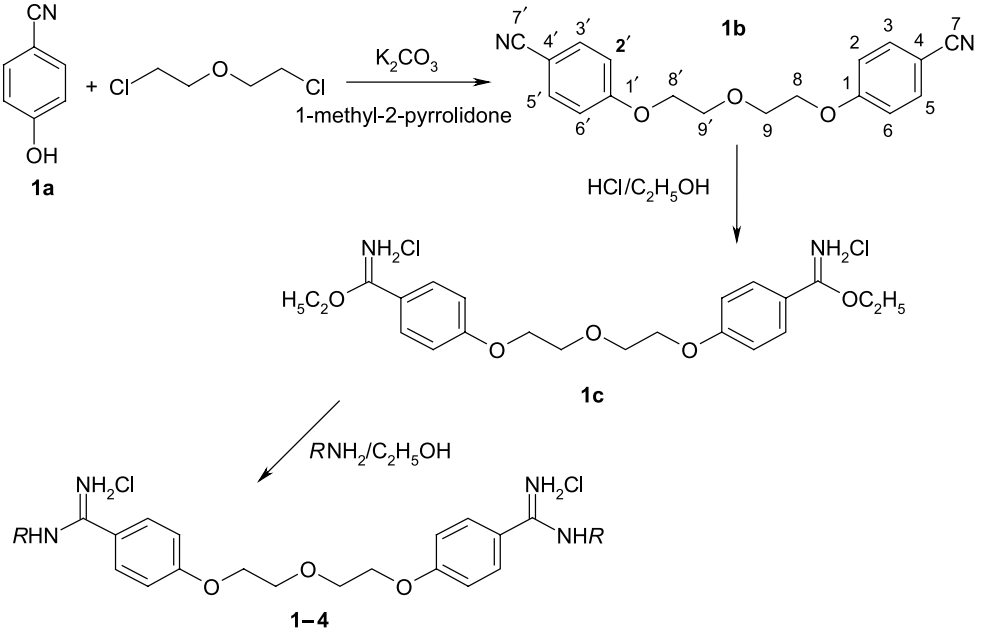

Scheme 1

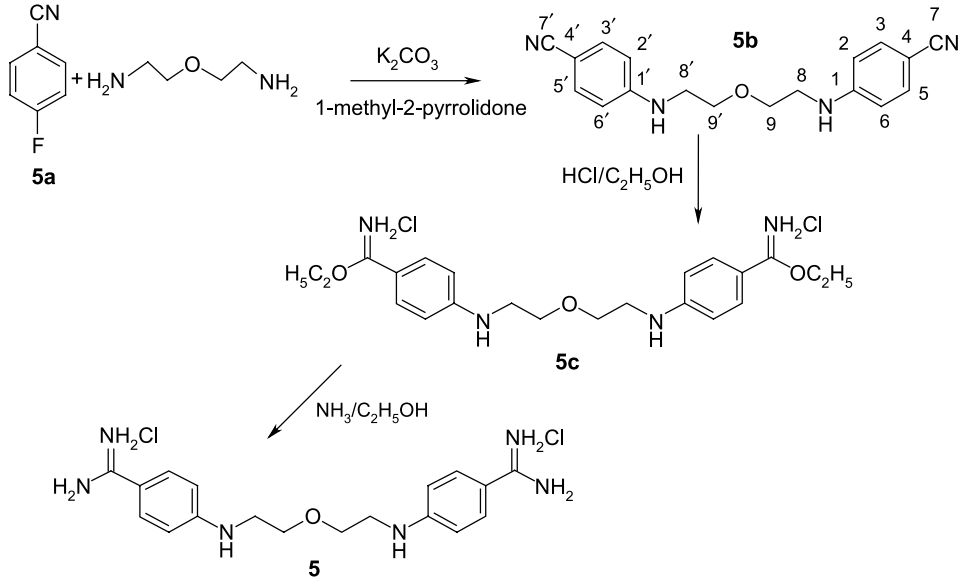

Scheme 2

refinement details are listed in Table 1, and hydrogen bonding parameters are given in Table 2. A perspective view of the molecular conformation, together with the atom numbering scheme, is shown in Fig. 2 (for drawing method see Ref. [18]).

1,5-Bis(4-amidinophenoxy)-3-oxapentane (γ-oxapentamidine, **1**) crystallizes from water solution as the dihydrochloride dihydrate salt in the monoclinic space group $C2/c$. The central O10 atom is located at two-fold crystallographic axis and the asymmetric unit contains one half of the molecule, one chloride ion, and one water molecule.

The crystal structures of only several aromatic diamidines derivatives related to pentamidine have been reported [19–21]. Apart from the crystal structures of the complexes of propamidine, pentamidine, γ-oxapentamidine, berenil and its furan derivatives and the *DNA* dodecamer d(*CGCGAATTCGCG*)$_2$ have been determined [9–11, 22]. These investigations indicate that the amidinium group of the drug could form H-bonded interactions with acceptor atoms of either adenine or thymine bases in the minor groove.

γ-Oxapentamidine contains an ether linkage in place of the more sterically bulky central methylene unit of pentamidine. All bond angles and distances within the structure of **1** are normal. Two aromatic rings are twisted by 19.45(5)° with respect to each other, with the dihedral angle between the plane of the phenyl ring and its neighbouring amidinium plane being 13.72(7)° as compared with 3–29° for related compounds.

The polyether linker of **1** adopts a folded conformation but in the crystal structure of the complex of γ-oxapentamidine and *DNA* a stretch of the central chain was found [10]. Such a conformation of **1** is probably due to molecular packing and intermolecular C–H$\cdots$O hydrogen bonds. The extended conformation of the central chain of γ-oxapentamidine in the complex with *DNA* may be a major factor in the positioning of the drug along the minor groove. So, our structure reveals a considerable flexibility of the polyether chain.

Table 1. Crystal data, data collection, and structure refinement for **1**

Compound	**1**
Empirical formula	$C_{18}H_{28}Cl_2N_4O_5$
Formula weight	451.34
T/K	296(2)
Wavelength/Å	0.71073
Crystal system, space group	monoclinic, $C\ 2/c$
Unit cell dimensions	
a/Å	22.700(1)
b/Å	10.2261(6)
c/Å	9.6042(5)
β/°	101.265(4)
Volume/Å^3	2186.5(2)
Z, D_x/Mg/m^3	4, 1.371
μ/mm^{-1}	0.333
$F(000)$	952
θ-range for data collection/°	3.20–29.93
hkl range	$-31 \leq h \leq 29$
	$-7 \leq k \leq 14$
	$-13 \leq l \leq 13$
Reflections:	
collected	10425
unique (R_{int})	2924(0.022)
observed ($I > 2\sigma(I)$)	2497
Data/restraints/parameters	2924/0/151
Goodness-of-fit on F^2	1.068
$R(F)$ ($I > 2\sigma(I)$)	0.0351
$wR(F^2)$ (all data)	0.1000
Max/min. $\Delta\rho$ (e/Å^3)	0.326/−0.288

Table 2. Hydrogen-bonding geometry (Å and deg.) for **1**

	1			
D–H···A	d(D–H)	d(H···A)	d(D···A)	<(DHA)
OW–H2W···Cl^{i}	0.82(2)	2.38(2)	3.204(1)	177(2)
N11–H11A···Cl^{ii}	0.80(2)	2.49(2)	3.264(1)	163(2)
N11–H11B···Cl^{iii}	0.88(2)	2.50(2)	3.313(1)	155(2)
N12–H12B···Cl^{iii}	0.82(2)	2.56(2)	3.323(1)	154(2)
N12–H12A···OW^{iv}	0.84(2)	2.05(2)	2.865(2)	164(2)
OW–H1W···Cl^{v}	0.81(2)	2.39(2)	3.196(1)	172(2)
C8–H8B···OW^{i}	0.97	2.68	3.509(2)	144
C5–H5···OW^{iv}	0.93	2.67	3.535(2)	154
C6–H6···O(8)^{iv}	0.93	2.69	3.610(1)	170
C6–H6···O10^{iv}	0.93	2.68	3.311(2)	126

Symmetry codes: (i) $-x, y, -z-1/2$; (ii) $x, -y+1, z+1/2$; (iii) $-x+1/2, -y+3/2, -z+1$; (iv) $-x, -y+2, -z$; (v) $-x, -y+1, -z$

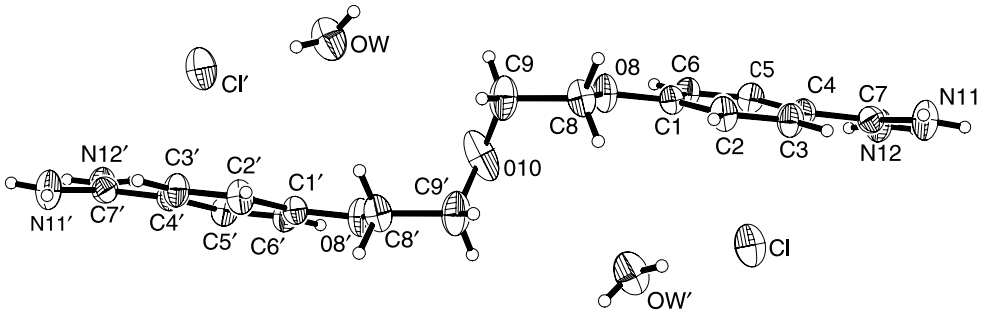

Fig. 2. A perspective view of the molecular conformation of **1** together with the atom numbering scheme

The crystal structure of **1** is stabilized by a number of hydrogen bonds (Table 2) involving the γ-oxapentamidine, water molecules, and chloride ions. The molecular packing and hydrogen bonding scheme in the crystal structure are depicted in Fig. 3. Thus, within the crystal, the molecules of γ-oxapentamidine are linked *via* C6–H6$\cdots$O8 and C6–H6$\cdots$O10 interactions (Table 2) to form columns along the *z* axis. Also, the water molecules and the chloride ions, *via* OW–H1W$\cdots$Cl and

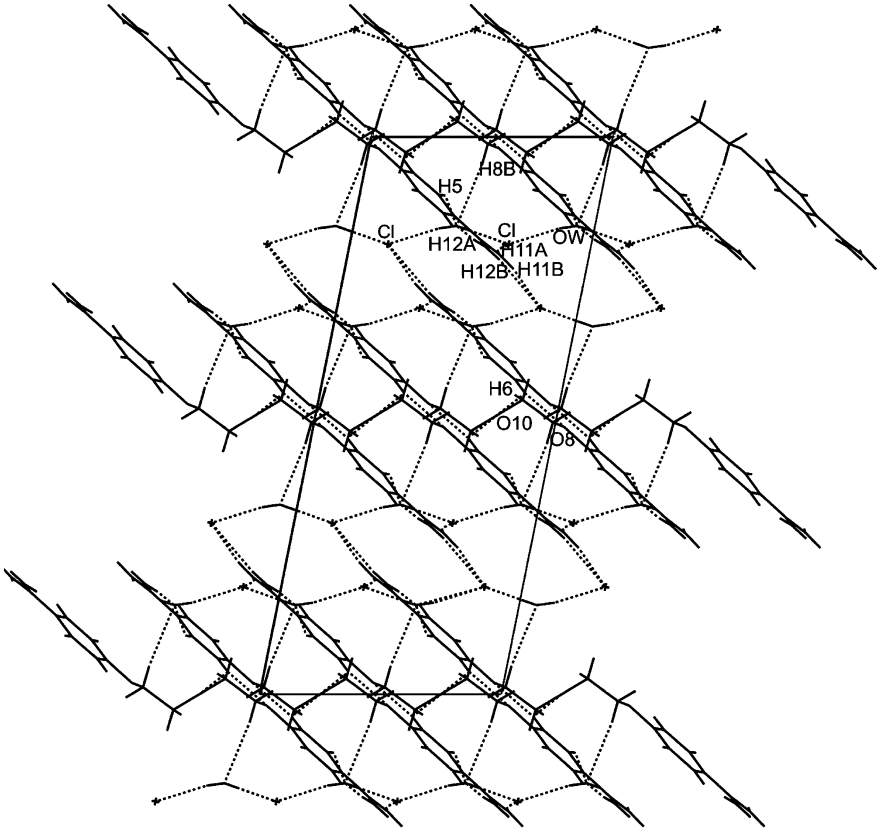

Fig. 3. Perspective drawing of the packing arrangement of **1** along the *b*-axis with dashed lines indicating the hydrogen bonding scheme

OW–H2W···Cl hydrogen bonds, create infinite chains along both sides of the columns. Adjacent columns and chains are further linked by N11–H11A···Cl, N12–H12A···OW hydrogen bonds and weaker interactions C5–H5···OW and C8–H8B···OW and in consequence wide bands are formed. The three-dimensional supramolecular structure results from combination of the bands *via* N11–H11B···Cl and N12–H12B···Cl hydrogen bonds.

^{13}C CP/MAS NMR Spectra in the Solid State

The ^{13}C CP/MAS NMR spectroscopy in the solid state is a complementary tool to the X-ray diffraction method. Of special interest is its application to the investigation of polymorphism and dynamic events of biologically active compounds in the solid state [23]. It was also of interest to obtain more structural information on those molecules for which we have no XRD data. The notation used in the discussion of the NMR results is illustrated in Fig. 1. Assignments of ^{13}C resonances in solid state were made from comparison with their solution spectra, and with the spectra of structurally related *para*-substituted benzenes. Theoretical shielding constants computed for geometries optimized at DFT level of theory for bis-amidines **1**–**5**, as well as for bis-nitriles **1b** and **5b**, and for X-ray derived atomic coordinates of **1** were used as an aid to the analysis of the more complicated spectral pattern. The ^{13}C CP/MAS NMR spectra of **1**–**5**, and of **1b** and **5b** are shown in Figs. 4 and 5, and the most probable assignments of signals are given in Table 3.

The central O ether atom incorporated in **1**–**5** formally dissects these molecules into two halves. For equivalent pairs of atoms from both parts of the molecule we could expect a different pattern of resonances in the solid state spectra depending on conformational equilibria. Surprisingly, not many differences were found as we compared ^{13}C atom signals of the aliphatic groupings in solutions and the solid state (*i.e.* there are single, and/or partially broadened ones). We have observed more significant differences only for aromatic carbons: the asymmetric non-averaged resonances in the spectra of bis-diamidines **1**, **5**, and bis-nitriles **1b**, **5b**. The separations of resonances of the *ortho* pairs C2, C6 (C2′, C6′) atoms and *meta* pairs C3, C5 (C3′, C5′) atoms are equal to 5–11 ppm and 1–2 ppm. It has been reported previously [24, 25] that benzene rings may exhibit different degrees of mobility dependent on intermolecular interactions and the nature of substituents present at C atoms. Both carbon atoms *ortho* to alkoxy or amino linkers are shielded in different ways: lone electron pairs of oxygen or nitrogen atoms pointing to the corresponding C atoms result in a high field shift of their resonances [26, 27]. The separations of signals of *meta* carbons are much smaller indicating that amidine and nitrile moieties are almost coplanar with the benzene rings in **1**, **1b**, and **5b**. Besides, in the spectrum of **5** we observed different resonances of C atoms in both benzene rings indicating that the ring planes are slightly twisted relative to all another. All those facts could indicate the lack of benzene and chain linker motions of **1**, **5**, **1b**, and **5b** in solid state.

In the spectra of **2**–**4** the aromatic C2, C6 and C3, C5 pairs of peaks broaden and become indistinct. Similarly, in the spectra of **3** and **4** the alkyl C8 (C8′), C9 (C9′) atoms resonances broadened. This was interpreted with a reorientation of those

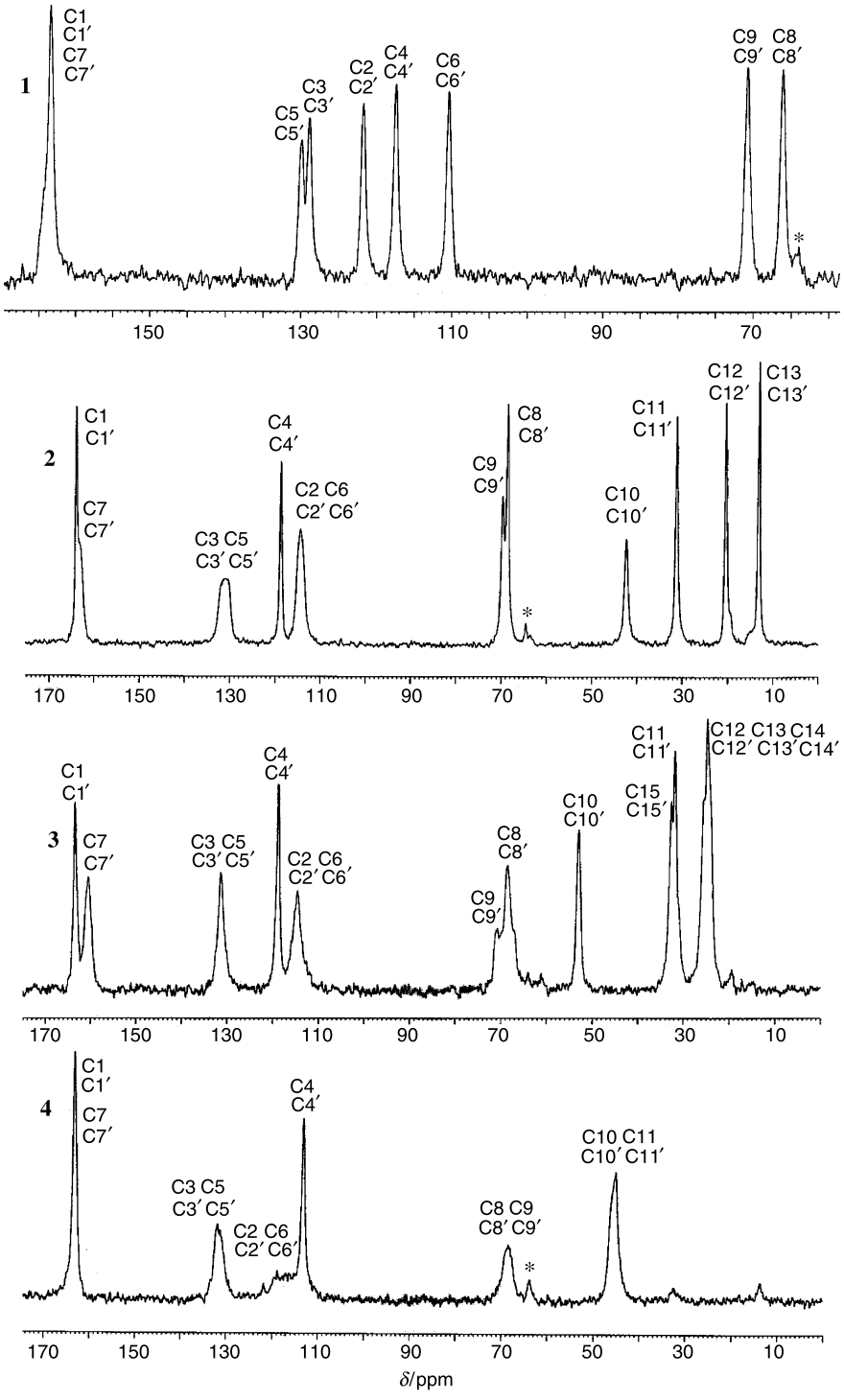

Fig. 4. The ^{13}C CP/MAS NMR spectra of **1–4** in the solid state

parts of molecules. The resonances of C atoms of both butyl chains (C10–C13 and C10′–C13′) in **2** are sharp singlets, thus demonstrating similarities in the chain conformations.

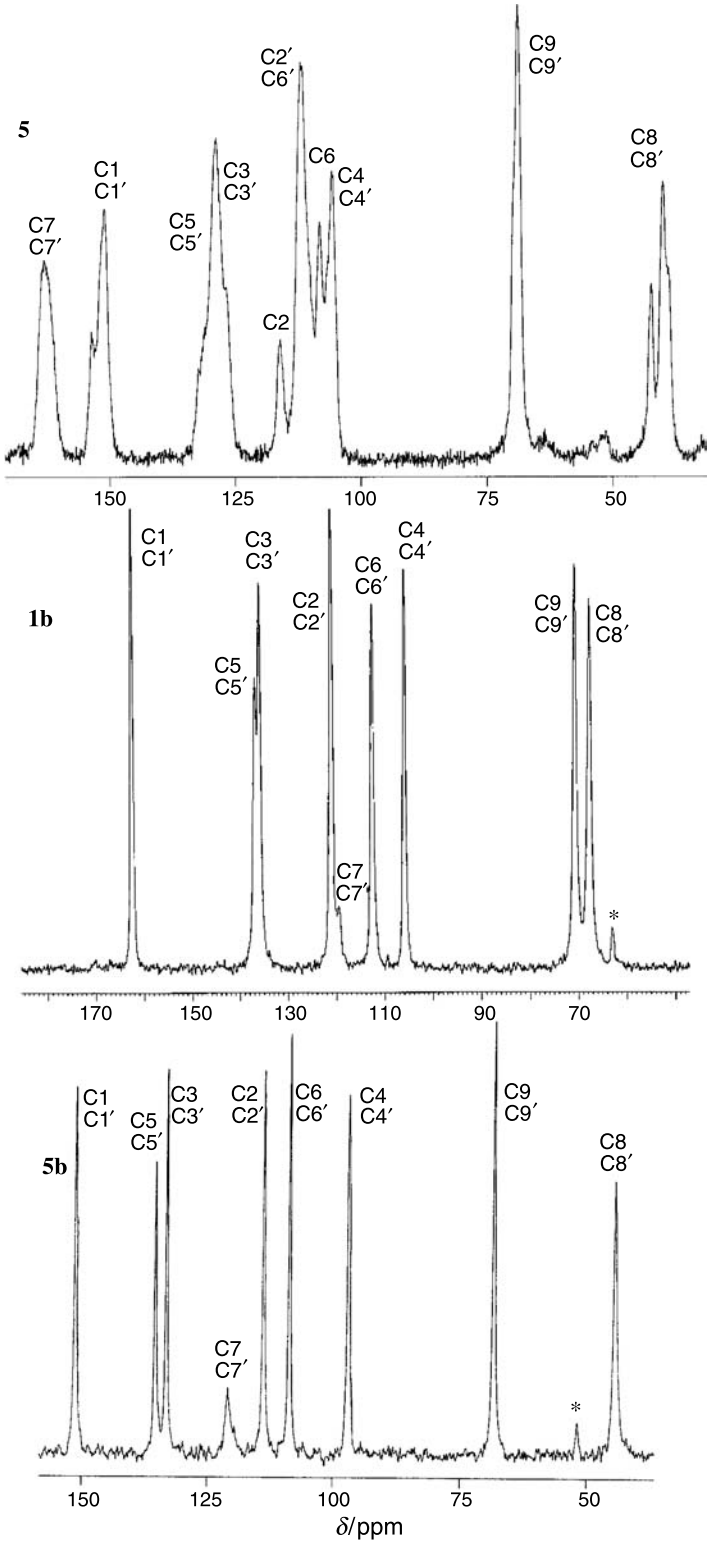

Fig. 5. The ^{13}C CP/MAS NMR spectra of 1,5-bis[(4-amidinophenyl)amino]-3-oxapentane dihydrochloride **5**, **1b**, and **5b** in the solid state

Table 3. Assignments of resonances in the ^{13}C CP/MAS NMR spectra of **1–5**, **1b**, and **5b**

No.	^{13}C chemical shifts in solid state/ppm									
	C1, C1′	C2, C2′	C3, C3′	C4, C4′	C5, C5′	C6, C6′	C7, C7′	C8, C8′	C9, C9′	C10, C10′; C11, C11′; C12, C12′; C13, C13′; C14, C14′; C15, C15′
1	163.4	121.8	129.9	117.5	128.9	110.4	163.4	66.2	70.8	–
2	163.9	114.3	130.8	118.7	130.8	114.3	163.9	68.6	69.6	42.3; 31.2; 20.4; 13.1
3	163.4	114.6	131.4	118.8	131.4	114.6	160.5	68.5	70.8	53.0; 31.9; 24.6; 26.6; 24.8; 31.9
4	163.3	113.2	131.8	118.9	131.8	113.2	163.3	68.5	68.5	45.2; 45.2
5	151.2	116.1; 112.1	128.9	105.9; 105.6	128.9	108.3; 112.1	162.7	40.0	69.0	–
1b	162.4	120.9	135.4	105.9	136.7	112.5	119.5	68.7	70.7	
5b	151.3	113.8	135.4	97.0	133.1	108.6	120.9	44.5	68.4	–

The resonances of C8 (C8′) in **5**, and imidazoline C11, C12 (C11′, C12′) atoms proximal to N atoms are broadened and/or splitted into unequal doublets (or quartets) due to residual coupling to quadrupolar ^{14}N [28]. In the spectra of bis-nitriles **1b** and **5b** the resonances of C atoms from nitrile groups are broadened. The water molecules, which were detected by X-ray measurement and elemental analyses, might influence the mobility of more hydrated molecules in the solid state.

Computation Results

The DFT method was used to study the geometries and NMR resonances of compounds **1–5**, **1b**, and **5b**. We have analyzed folded and extended 'zig-zag'

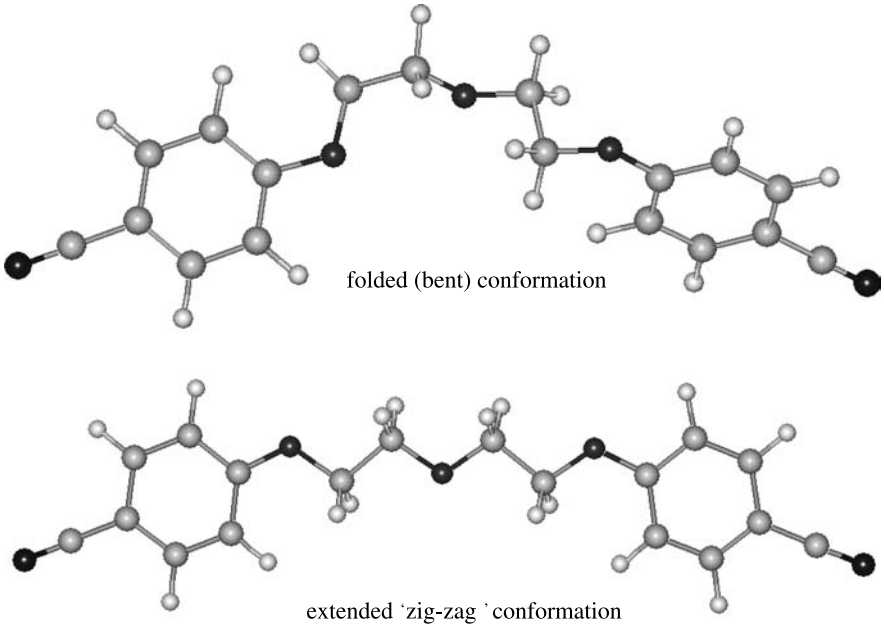

Fig. 6. Hypothetical conformations in solid state (folded and extended) shown for **1b**

conformations of the ether linkage (see examples shown in Fig. 6), and we found that for bis-amidines the folded (bent) conformations are slightly more stable. For **1b** the extended conformation is slightly preferred by 10.5 kJ/mol, but for **5b**, the folded one is more stable by 7.5 kJ/mol. These differences are not significant and could not be decisive for the preferred structure in the solid state where the intermolecular interactions play a meaningful role. Thus, we decided to compute the NMR shielding constants for the atomic coordinates corresponding to both folded and extended conformations, and to compare them with the experimental chemical shifts of C atoms in the solid state NMR spectra. The calculated shielding constants for equivalent pairs of C atoms were the same in extended conformations, but slightly different for folded ones (on average by 0.2 ppm for the ether linkage, and 1 ppm for the aminoether). Next, we analyzed the correlation coefficients r^2 for the correlations between the calculated shielding constants σ (for both conformations of the linker) and the experimental chemical shifts δ. We obtained linear correlations with r^2 values between 0.982 to 0.997. The correlation coefficients were higher for the structures with folded linker for **1**–**5**, and with the extended one for **1b** and **5b**. Simultaneously, using the same method we computed the shielding constants for the crystallographic coordinates of **1**. The calculated shielding constants for the X-ray geometry of **1** are slightly different from those for the DFT geometry of **1** with folded linker, but in both cases linear correlations were found (see Fig. 7). The above finding is good evidence that linear correlations between the computed shielding constants for DFT geometries and the experimental chemical shifts could be used to characterize the molecular structure of the studied compounds. However, the resonances in the spectra of **2**–**5** are broad and this gave rise to some uncertainty. We ventured a guess of the favored solid-state conformations only for **1b** and **5b**, the spectra of which are sharp: for both we propose extended 'zig–zag' conformations (see Fig. 6).

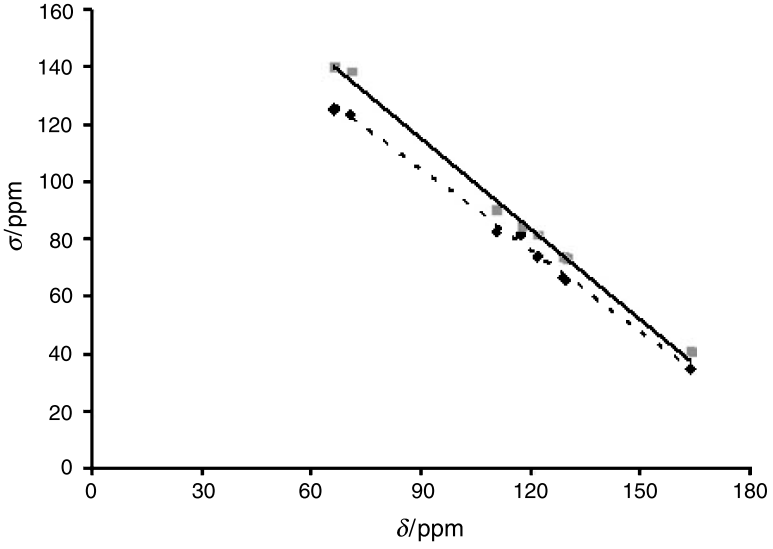

Fig. 7. Linear correlations between calculated shielding constants σ and experimental chemical shifts δ for **1**: - - - - - for DFT structure, $r^2 = 0.997$; — for X-ray structure, $r^2 = 0.996$

Table 4. The percent of test cell growth relative to control cell growth ($T/C \cdot 100\%$) for **1**–**4**

Compounds ($c = 1 \cdot 10^{-4}\,M$)	Human tumor cell lines		
	MCF-7	NCI-H460	SF-298
1	57	32	55
2	52	49	45
3	48	50	46
4	114	112	72

Preliminary Anticancer Assay

Compounds **1**–**5** were accepted for evaluation by the Division of Cancer Treatment and Diagnosis, National Cancer Institute (Bethesda, USA) in a 3-cell line panel, consisting of the MCF7 (breast), NCI-H460 (lung), and SF-268 (CNS) cells. The details are available at the web site http://dtp.nci.nih.gov. The results are reported in Table 4 as the percentage of growth of the treated cells compared with untreated control cells. Substitution of the amidino groups of **1** by alkyl or 4,5-dihydroimidazoline moieties gave compounds that were less potent relative to the unsubstituted analog. Up to now, only **1** was scheduled for evaluation against the full panel of 60 tumor cell lines. It inhibits 50% of growth of human leukemia CCRF-CEM cell line at a concentration of $1 \cdot 10^{-6}\,M$. Its cytotoxicity against the remaining cancer cell lines (non-small cell lung, colon, CNS, melanoma, ovarian, renal, prostate, breast) was much lower. Compound **5** is still in testing.

Conclusions

The reported series of pentamidine analogs was synthesized in sufficient yields. In the ^{13}C CP/MAS NMR spectra of bis-amidines **1** and **5** and in both bis-nitriles **1b** and **5b** we observed distinct resonances of aromatic carbons, which could be evidence of the absence of intramolecular motions in solid state. That was not the case for N-alkylated bis-amidines **2**–**4**. We have not observed the resonance pattern (*e.g.* double signals), which could be explained in terms of polymorphism.

In the crystal the molecules of **1** are organized into a three-dimensional network by different intermolecular interactions. The crystal structural analysis lends support to the role of hydrogen bonds in influencing the conformation of the γ-oxapentamidine and the crystal packing.

The bis-amidines **1**–**3** at $1 \cdot 10^{-4}\,M$ reduce the growth of MCF7 (breast), NCI-H460 (lung), and SF-268 (NCS) cells on average by 48%. Compound **1** inhibits 50% of growth of a human leukemia CCRF-CEM cell line at $1 \cdot 10^{-6}\,M$.

Experimental

All chemicals were purchased from the major chemical suppliers as high or highest purity grade and used without any further purification. Melting points were determined with a Digital Melting Point Apparatus 9001. ^{1}H and ^{13}C NMR spectra in solution were recorded at 25°C with a Varian Unity plus-200, and standard Varian software was employed. Several (as indicated) ^{1}H NMR and ^{13}C NMR

spectra in solution were recorded with a Bruker Avance DMX 400. The solid state ^{13}C CP/MAS NMR spectra were measured using a Bruker Avance DMX 400. A powdered sample was spun at 8 kHz. Contact time of 4 ms, repetition time of 10 s, and spectral width of 24 kHz were used for accumulation of 3000 scans. Chemical shifts δ/ppm were referenced to *TMS*. Elemental analyses were averaged from two independent determinations and agreed favourably with the calculated values. Prefabricated silica gel sheets (Merck Kieselgel 60 F_{254}) were used for TLC.

1,5-Bis(4-cyanophenoxy)-3-oxapentane (**1b**) [15]
4-Hydroxybenzonitrile (**1a**, 1.20 g, 10 mmol) and 0.72 g bis(2-chloroethyl)ether (5 mmol) were added to 15 cm^3 1-methyl-2-pyrrolidone together with 2.08 g anh. K_2CO_3 (15 mmol). The mixture was allowed to stand at 130°C for 2 h while stirring. The resulting hot solution was added to 200 cm^3 cold H_2O. The formed solid was filtered off and washed with H_2O. The precipitate was recrystallized from absolute ethanol to give 1.18 g (78%) of sandy crystals. Mp 136–137°C (Ref. [15]: 134–135°C); ^1H NMR (400 MHz, $CDCl_3$): $\delta = 3.94$ (t, $J = 4.8$ Hz, 9-H_2, 9′-H_2), 4.19 (t, $J = 4.8$ Hz, 8-H_2, 8′-H_2), 6.94–6.96 (m, 2-H, 2′-H, 6-H, 6′-H), 7.56–7.58 (m, 3-H, 3′-H, 5-H, 5′-H) ppm; ^{13}C NMR (100 MHz, $CDCl_3$): $\delta = 67.90$ (8-C, 8′-C), 69.87 (9-C, 9′-C), 104.46 (4-C, 4′-C), 115.47 (2-C, 2′-C, 6-C, 6′-C), 119.31 (7-C, 7′C), 134.18 (3-C, 3′-C, 5-C, 5′-C), 162.14 (1-C, 1′-C) ppm; IR (KBr): $\bar{\nu} = 2218$, 1604, 1504, 1257 cm^{-1}.

1,5-Bis[(4-cyanophenyl)amino]-3-oxapentane (**5b**, $C_{18}H_{18}N_4O$)
A 0.78 g (51%) of yellowish crystals from absolute ethanol (mp 121.6–122.8°C) was obtained from 1.21 g **5a** (10 mmol) and 0.885 g 1,5-diamino-3-oxapentane dihydrochloride (5 mmol) with 5.53 g anh. K_2CO_3 (40 mmol) by the procedure described above. ^1H NMR (400 MHz, $CDCl_3$): $\delta = 3.35$ (q, $J = 4.8$ Hz, 8-H_2, 8′-H_2), 3.71 (t, $J = 4.8$ Hz, 9-H_2, 9′-H_2), 4.69 (br s, NH), 6.55–6.57 (m, 2-H, 2′-H, 6-H, 6-H′), 7.38–7.40 (m, 3-H, 3′-H, 5-H, 5′-H) ppm; ^{13}C NMR (100 MHz, $CDCl_3$): $\delta = 42.54$ (8-C, 8′-C), 69.09 (9-C, 9′-C), 98.44 (4-C, 4′-C), 112.20 (2-C, 2′-C, 6-C, 6′-C), 120.45 (7-C, 7′C), 133.54 (3-C, 3′-C, 5-C, 5′-C), 151.20 (1-C, 1′-C) ppm; IR (KBr): $\bar{\nu} = 3360$, 2210, 1605, 1524 cm^{-1}.

1,5-Bis[4-(ethoxyiminoyl)phenoxy]-3-oxapentane dihydrochloride (**1c**, $C_{22}H_{28}N_2O_5 \cdot 2HCl$)
To 25 cm^3 absolute ethanol saturated with dry HCl 1.54 g 1,5-bis(4-cyanophenoxy)-3-oxapentane (5 mmol) were added. The solution was kept at ambient temperature for 24 h in a sealed vessel. Anhydrous ether was then added until complete precipitation was attained. The precipitate was quickly filtered off (avoiding prolonged suction) and dried under reduced pressure giving the very hygroscopic HCl salt in nearly quantitative yield. The crude product was used in the next step without additional purification.

1,5-Bis(4-amidinophenoxy)-3-oxapentane dihydrochloride (**1**) [15]
The crude **1c** was added to 25 cm^3 absolute ethanol saturated with anh. NH_3, and the mixture was stirred at ambient temperature for 24 h in a sealed vessel. The solvent was evaporated under reduced pressure and the residue was stirred with aqueous NaOH (1 g NaOH in 30 cm^3 H_2O) for 0.5 h. The precipitated white solid was filtered off and washed with cold H_2O. The free base was converted to its HCl salt by refluxing with an ethanolic solution of HCl (20 cm^3 absolute ethanol and 2.5 cm^3 17.7% aqu. solution of HCl in absolute ethanol) until complete dissolution of the solid was achieved. Anhydrous ether (40 cm^3) was added to this clear solution at ambient temperature. The precipitate was filtered off, washed with ether, and dried at 60°C for 2 h to give 1.20 g white solid (57%). Mp 258–260°C (Ref. [15]: 256–258°C); ^1H NMR (200 MHz, *DMSO-d_6*): $\delta = 3.86$ (br s, 9-H_2, 9′-H_2), 4.26 (br s, 8-H_2, 8′-H_2), 7.14–7.19 (m, 2-H, 2′-H, 6-H, 6′-H), 7.88–7.93 (m, 3-H, 3′-H, 5-H, 5′-H), 9.22 (br s, NH_2), 9.32 (br s, NH_2) ppm; ^{13}C NMR (50.3 MHz, *DMSO-d_6*): $\delta = 67.6$ (8-C, 8′-C), 68.7 (9-C, 9′-C), 114.7 (2-C, 2′-C, 6-C, 6′-C), 119.4 (4-C, 4′-C), 130.1 (3-C, 3′-C, 5-C, 5′-C), 162.7 (1-C, 1′-C), 164.6 (7-C, 7′-C) ppm. IR (KBr): $\bar{\nu} = 3418$, 3325, 3151.5, 1682, 1663, 1609, 1489, 1273 cm^{-1}.

1,5-Bis[4-(N-butylamidino)phenoxy]-3-oxapentane dihydrochloride
(**2**, $C_{26}H_{38}N_4O_3 \cdot 2HCl \cdot ½H_2O$)
A suspension of **1c** and 1.60 g butylamine (22 mmol) was stirred in 25 cm^3 absolute ethanol at ambient temperature for 72 h. Workup was the same as described above to give 1.42 g white solid (55%). Mp 241–242°C; ^{1}H NMR (200 MHz, *DMSO-d_6*): $\delta = 0.92$ (t, $J = 7.4$ Hz, 13-H_3, 13′-H_3), 1.29–1.47 (m, 12-H_2, 12′-H_2), 1.55–1.70 (m, 11-H_2, 11′-H_2), 3.38–3.51 (m, a signal of water included, 10-H_2, 10′-H_2), 3.83–3.88 (m, 9-H_2, 9′-H_2), 4.22–4.26 (m, 8-H_2, 8′-H_2), 7.12–7.16 (m, 2-H, 2′-H, 6-H, 6′-H), 7.79–7.83 (m, 3-H, 3′-H, 5-H, 5′H), 9.08 (br s, NH), 9.44 (br s, NH), 9.82 (br s, NH) ppm; ^{13}C NMR (50.3 MHz, *DMSO-d_6*): $\delta = 13.5$ (13-C, 13′-C), 19.4 (12-C, 12′-C), 29.4 (11-C, 11′-C), 42.1 (10-C, 10′-C), 67.6 (8-C, 8′-C), 68.8 (9-C, 9′-C), 114.5 (2-C, 2′-C, 6-C, 6′-C), 120.5 (4-C, 4′-C), 130.1 (3-C, 3′-C, 5-C, 5′-C), 161.7 (7-C, 7′-C), 162.2 (1-C, 1′-C) ppm; IR (KBr): $\bar{\nu} = 3044$, 2932, 2874, 1674.1, 1609, 1508, 1269 cm^{-1}.

1,5-Bis[4-(N-cyclohexylamidino)phenoxy]-3-oxapentane dihydrochloride
(**3**, $C_{30}H_{42}N_4O_3 \cdot 2HCl \cdot 2½H_2O$)
A white solid (0.98 g, 32%) was obtained from **1c** and 1.98 g cyclohexylamine (20 mmol) by the procedure described above. Mp 291–292°C (dec); ^{1}H NMR (200 MHz, *DMSO-d_6*): $\delta = 1.10$–1.88 (m, cyclohexyl protons), 3.85 (br s, 9-H_2, 9′-H_2), 4.23 (br s, 8-H_2, 8′-H_2), 7.10–7.14 (m, 2-H, 2′-H, 6-H, 6′-H), 7.75–7.79 (m, 3-H, 3′-H, 5-H, 5′-H) ppm; ^{13}C NMR (50.3 MHz, *DMSO-d_6*): $\delta = 24.2$ (13-C, 13′-C), 24.7 (12-C, 12′-C, 14-C, 14′-C), 31.1 (11-C, 11′-C, 15-C, 15′-C), 51.6 (10-C, 10′-C), 67.6 (8-C, 8′-C), 68.8 (9-C, 9′-C), 114.4 (2-C, 2′-C, 6-C, 6′-C), 121.2 (4-C, 4′-C), 130.2 (3-C, 3′-C, 5-C, 5′-C), 160.7 (7-C, 7′-C), 162.0 (1-C, 1′-C) ppm; IR (KBr): $\bar{\nu} = 3036$, 2932, 2858, 1670, 1609, 1512, 1261 cm^{-1}.

1,5-Bis[4-(4,5-dihydro-2-imidazoyl)phenoxy]-3-oxapentane dihydrochloride
(**4**, $C_{22}H_{22}N_4O_3 \cdot 2HCl \cdot 3H_2O$)
A suspension of **1c** and 1.20 g ethane-1,2-diamine (20 mmol) was refluxed in 25 cm^3 absolute ethanol for 24 h. After workup described for **1** 2.10 g cream solid (80%) were obtained. Mp 89–90°C; ^{1}H NMR (200 MHz, *DMSO-d_6*): $\delta = 3.36$ (s, 10-H_2, 10′-H_2, 11-H_2, 11′-H_2), 3.83–3.87 (m, 9-H_2, 9′-H_2), 4.24–4.28 (m, 8-H_2, 8′-H_2), 7.17–7.22 (m, 2-H, 2′-H, 6-H, 6-H′), 8.02–8.07 (m, 3-H, 3′-H, 5-H, 5′-H), 10.60 (s, NH) ppm; ^{13}C NMR (50.3 MHz, *DMSO-d_6*): $\delta = 44.0$ (10-C, 10′-C, 11-C, 11′-C), 67.7 (8-C, 8′-C), 68.7 (9-C, 9′-C), 114.0 (4-C, 4′-C), 115.0 (2-C, 2′-C, 6-C, 6′-C), 130.9 (3-C, 3′-C, 5-C, 5′-C), 163.1 (7-C, 7′-C), 163.8 (1-C, 1′-C) ppm;. IR (KBr): $\bar{\nu} = 3317$, 3128, 1651, 1612, 1504 cm^{-1}.

1,5-Bis[(4-amidinophenyl)amino]-3-oxapentane dihydrochloride (**5**, $C_{18}H_{24}N_6O \cdot 2HCl \cdot ½H_2O$)
A 1.29 g (61% yield) beige solid (mp 288–292°C (dec)) was obtained from **5b** by the procedure described for **1**. ^{1}H NMR (400 MHz, *DMSO-d_6*): $\delta = 3.30$ (t, $J = 5.0$ Hz, 8-H_2, 8′-H_2), 3.61 (t, $J = 5.0$ Hz, 9-H_2, 9′-H_2), 5.16 (br s, NH), 6.73–6.75 (m, 2-H, 2′-H, 6-H, 6-H′), 7.70–7.73 (m, 3-H, 3′-H, 5-H, 5′-H), 8.75 (s, NH), 8.91 (s, NH) ppm;^{13}C NMR (100 MHz, *DMSO-d_6*): $\delta = 42.18$ (8-C, 8′-C), 68.60 (9-C, 9′-C), 111.20 (2-C, 2′-C, 6-C, 6′-C), 112.10 (4-C, 4′-C), 129.73 (3-C, 3′-C, 5-C, 5′-C), 153.56 (1-C, 1′-C), 164.29 (7-C, 7′C) ppm; IR (KBr): $\bar{\nu} = 3317$, 3128, 1651, 1612, 1504 cm^{-1}.

X-Ray Diffraction Studies
An X-ray quality crystal of 1,5-bis(4-amidinophenoxy)-3-oxapentane (γ-oxapentamidine, **1**) was obtained from water solution as the dihydrochloride dihydrate salt by slow evaporation. Diffraction data were collected on an Oxford Diffraction KM4CCD diffractometer [29] at 296 K, using graphite-monochromated MoK_α radiation. A total of 782 frames were measured in six separate runs. The ω-scan was used with a step of 0.75°, two reference frames were measured after every 50 frames, they did not show any systematic changes either in peaks' positions or in their intensities. The unit cell parameters were determined by least-squares treatment of setting angles of 5749 highest-intensity

reflections chosen from the whole experiment. Intensity data were corrected for *Lorentz* and polarization effects [30]. The structures were solved by direct methods with the SHELXS-97 program [31] and refined with full-matrix least-squares by the SHELXL-97 program [32]. The function $\Sigma w(|F_o|^2 - |F_c|^2)^2$ was minimized with $w^{-1} = [\sigma^2(F_o)^2 + (0.0511P)^2 + 1.1072P]$, where $P = ({F_o}^2 + 2{F_c}^2)/3$. All non-hydrogen atoms were refined with anisotropic thermal parameters. The coordinates of the hydrogen atoms involved in hydrogen bonds N–H···Cl, N–H···O, O–H···Cl, namely H11A, H11B, H12A, H12B, H1W, and H2W were found in difference *Fourier* synthesis and their positional parameters were refined. The positions of the other hydrogen atoms were generated geometrically and refined as a riding model. Thermal parameters of all hydrogen atoms were calculated as 1.2 times U_{eq} of the respective carrier carbon atom. An empirical extinction correction was also applied according to the formula ${F_c}' = kF_c[1 + (0.001\chi {F_c}^2\lambda^3/\sin 2\theta)]^{-1/4}$ [32], and the extinction coefficient χ was equal to 0.0039(6). Crystallographic data were deposited at the Cambridge Crystallographic Data Center as supplementary publications No CCDC 600091.

Molecular Modelling

Both crystallographic and optimized atom coordinates for **1** and only optimized for **2–5**, **1b**, and **5b** were used for computation of shielding constants σ/ppm of ^{13}C atoms to assign the resonances in solid-state NMR spectra. We have employed the DFT method with B3LYP/6-311 + (d,p) hybrid functional for structure optimization of cations of **1–5**, and B3LYP/6-31G(d,p) for neutral molecules **1b** and **5b**, and the CHF–GIAO approach for the NMR shielding constants computations using the Gaussian 98 program [33].

References

[1] Stephens CE, Farisl T, Kim S, Wilson WD, Schell WS, Perfect JR, Franzblau SG, Boykin DW (2001) J Med Chem **44**: 1741, and references therein
[2] Queener SF (1995) J Med Chem **38**: 4739
[3] Fishman JA (1998) Antimicrob Agents Chemother **42**: 1309
[4] Neamati N, Mazumder A, Sunder S, Owen JM, Tandon M, Lawn JW, Pommier Y (1998) Mol Pharm **54**: 280
[5] Geratz JD, Cheng MC-F, Tidwell RR (1976) J Med Chem **19**: 634
[6] Reddy BS, Sondhi SM, Lown JW (1999) Pharmacol Ther **84**: 1
[7] Pathak MK, Dhawan D, Linder DJ, Borden EC, Farver C, Yi T (2002) Mol Cancer Ther **1**: 1255
[8] Puckowska A, Bielawski K, Bielawska A, Midura-Nowaczek K (2004) Eur J Med Chem **39**: 99
[9] Edwards K, Jenkins TC, Neidle S (1992) Biochemistry **31**: 7104
[10] Nunn CM, Jenkins TC, Neidle S (1994) Eur J Biochem **226**: 953
[11] Trent JO, Clark GR, Kumar A, Wilson WD, Boykin DW, Hall JE, Tidwell RR, Blagburn BL, Neidle S (1996) J Med Chem **39**: 4554
[12] Ashley JN, Barber HJ, Ewins AJ, Newbery G, Self ADH (1942) J Chem Soc: 103
[13] Berg SS, Newbery G (1949) J Chem Soc: 642
[14] Francesconi I, Wilson WD, Tanious FA, Hall JE, Bender BC, Tidwell RR, McCurdy D, Boykin DW (1999) J Med Chem **42**: 2260
[15] Chun-Chieh Ch'en, Ch'ang-sheng Sun, Hung-Ch'iang Sung, Ch'i-Chiech Chang (1959) Yaoxue Xuebao **7**: 149; Chem Abstr **54**: 5528 (1964)
[16] van Es T (1965) J Chem Soc: 1564
[17] Bogatskii W, Lukyanyenko NG, Kirichenko TI (1980) Zh Org Khim **16**: 1306
[18] Stereochemical Workstation Operation Manual. Release 3.4. (1989) Siemens Analytical X-ray Instruments Inc., Madison, Wisconsin, USA
[19] Lowe PR, Sansom CE, Schwalbe CH, Stevens MFG (1989) J Chem Soc Chem Commun **16**: 1164
[20] Srikrishnan T, De NC, Alam AS, Kapoor J (2004) J Chem Cryst **34**: 813

[21] Courseille C, Busetta B, Comberton G, Hospital M (1971) C R Acad Sci Ser C (Chim) **272**: 1115
[22] Nunn CM, Jenkins TC, Neidle S (1993) Biochemistry **32**: 13838
[23] Fyfe CA (1983) Solid State NMR for Chemists. CFC Press: Guelph Ontario, Canada, pp 30–71
[24] Saito H, Yokoi M, Aida M, Kodama M, Oda T, Sato Y (1988) Magn Reson Chem **26**: 155
[25] Fattah J, Twyman M, Heyes SJ, Watkin DJ, Edwards AJ, Prout K, Dobson CM (1993) J Am Chem Soc **115**: 5636
[26] Maciejewska D (1999) J Mol Struct **478**: 121
[27] Herold F, Maciejewska D, Wolska I (2000) J Phys Org Chem **13**: 1
[28] Olivieri AC, Frydman L, Diaz F (1987) J Magn Reson **75**: 50
[29] Oxford Diffraction Poland (2003) CrysAlisCCD, CCD data collection GUI, version 1.171
[30] Oxford Diffraction Poland (2003) CrysAlisRED, CCD data reduction GUI, version 1.171
[31] Sheldrick GM (1990) Acta Crystallogr **A46**: 467
[32] Sheldrick GM (1997) SHELXL97 Program for the Refinement of Crystal Structures, University of Göttingen, Germany
[33] Gaussian 98, Revision A.7 (1998) Frisch MJ, Trucks GW, Schlegel HB, Scuseria GE, Robb MA, Cheeseman JR, Zakrzewski VG, Montgomery JA Jr, Stratmann RE, Burant JC, Dapprich S, Millam JM, Daniels AD, Kudin KN, Strain MC, Farkas O, Tomasi J, Barone V, Cossi M, Cammi R, Mennucci B, Pomelli C, Adamo C, Clifford S, Ochterski J, Petersson GA, Ayala PY, Cui Q, Morokuma K, Malick DK, Rabuck AD, Raghavachari K, Foresman JB, Cioslowski J, Ortiz JV, Baboul AG, Stefanov BB, Liu G, Liashenko A, Piskorz P, Komaromi I, Gomperts R, Martin RL, Fox DJ, Keith T, Al-Laham MA, Peng CY, Nanayakkara A, Gonzalez C, Challacombe M, Gill PMW, Johnson B, Chen W, Wong MW, Andres JL, Gonzalez C, Head-Gordon M, Replogle ES, Pople JA, Gaussian Inc., Pittsburgh, PA

Verleger: Springer-Verlag GmbH, Sachsenplatz 4–6, 1201 Wien, Austria. – Herausgeber: Österreichische Akademie der Wissenschaften, Dr.-Ignaz-Seipel-Platz 2, 1010 Wien, und Gesellschaft Österreichischer Chemiker, Eschenbachgasse 9, 1010 Wien, Austria. – Redaktion: Getreidemarkt 9/163-OC, 1060 Wien, Austria. – Satz und Umbruch: Thomson Press Ltd., Chennai, India. – Offsetdruck: Manz Crossmedia, 1051 Wien, Austria. – Verlagsort: Wien. – Herstellungsort: Wien. – Printed in Austria.